

MATHEMATICAL MODEL OF FATIGUE DEGRADATION OF CYLINDRICAL PIEZO ELEMENT OF LINEAR MICRO PIEZO MOTOR

 Mehman Hasanov^{1*},  Sahib Piriev¹,  Konul Hacıyeva²,
 Turana Rasullu¹,  Emin Payizov¹

¹Azerbaijan Technical University, Baku, Azerbaijan

²Sumgait State University, Sumgait, Azerbaijan

Abstract. In the article, a mathematical model has been constructed and investigated by analyzing the problem of disintegration during torsion of the cylindrical shaped piezo element in the linear piezoelectric engine. Nonlinear differential equations expressing the expansion of the disintegration surface formed during the torsion of the piezo element under the influence of variable torsional moment have been formulated. Guidelines determining the initial degradation period for the development of the disintegration process have been obtained, and based on the developed mathematical model, displacement curves of the disintegration surface motion have been established.

Keywords: piezoelectric element, linear micro piezoelectric motor, mathematical model of piezoelectric element fatigue, mechanical oscillations.

Corresponding author: Mehman Hasanov, Department Radiotechnics and Telecommunication, Azerbaijan Technical University, Baku, Azerbaijan, Tel.: +994 70 211 22 83, e-mail: mehman.hasanov@aztu.edu.az

Received: 2 April 2024; Revised: 22 May 2024; Accepted: 1 June 2024; Published: 2 August 2024.

1 Introduction

Despite the creation of a large number of piezoelectric motors according to their constructive structure, application areas, output parameters and other indicators (Ryabtsov, 2013; Samarin, 2006; Vishnevsky et al., 1993; Hasanov et al., 2022; Hasanov & Gardashov, 2017; Hasanov et al., 2021; Hasanov, 2019, 2018; Gayvorovskaya & Rybalov, 2015), the construction and application of a new linear micro piezoelectric motor is one of the most important issues in the creation of high-precision and high-speed devices. For this purpose, a new controllable linear micro piezoelectric motor construction with high-precision linear motion in the micrometre range was proposed (Hasanov et al., 2022, 2021; Hasanov, 2019).

In (Ryabtsov, 2013; Hasanov et al., 2022; Hasanov, 2019), the linear micro piezoelectric motor intended for application in optical transmission communication devices and the schematics reflecting the structure of the piezoceramics that make up it were presented. The proposed linear micro piezoelectric motor consists of a motion guide element, a piezoelectric element in a cylindrical shape and other auxiliary parts.

Structurally, the piezo element of the linear micro piezoelectric motor is cylindrical and consists of longitudinal wave-feeding electrodes separated by the circumference and height of the cylinder. The construction of the cylindrical piezo element consists of electrodes that create

How to cite (APA): Hasanov, M., Piriev, S., Hacıyeva, K., Rasullu, T. & Payizov, E. (2024). Mathematical model of fatigue degradation of cylindrical piezo element of linear micro piezo motor. *Advanced Mathematical Models & Applications*, 9(2), 223-233 <https://doi.org/10.62476/amma9223>

transverse oscillations along the circumference of the cylinder and longitudinal oscillations along its height. Homonymic electrodes are connected and connected to a food source with a high resonance frequency. The resonance frequency of the food source should correspond to the resonance frequency of mechanical oscillations (Hasanov, 2019; Hasanov et al., 2024).

The working principle of the mentioned linear micro piezoelectric motor is obtained as a result of the combined effect of both oscillations. As a result, as a result of both mechanical oscillations (height and width), the same points of the cylindrical piezo element are simultaneously excited by two types of oscillations. The study of the working characteristics of the cylindrical piezo element of the linear micro piezoelectric motor working with the mentioned principle, including its fatigue, is one of the most relevant issues for piezoelectric motors.

2 Essence analysis of fatigue degradation of piezoelectric elements

As it can be seen if two oscillations are used in both cases, including excitation with longitudinal waves along the height of the cylinder, the amplitude of transverse mechanical oscillations increases by 2-3 times. However, depending on the working process, the mechanical stresses caused by tension and torsion in the cylindrical piezo elements used in piezoelectric motors change their value and direction. Therefore, the period of stress caused by external forces whose value changes depending on time is called stress.

Experience indicates that piezo elements whose strength is not broken in the first cycle of loading can be broken when the number of loading cycles reaches a certain value, that is, the strength of the piezo element depends on the number of operating cycles.

The strength limit of piezo elements working under the influence of repeatedly changing mechanical stresses is much smaller than the strength limit in the case where the stresses do not change. The essence of the fatigue degradation caused by such stresses is as follows:

- Microcracks invisible to the naked eye appear as a result of constructive, structural or technological factors in the zone where the greatest stresses are generated in the case of fatigue degradation of piezo elements;
- With a long-term change of voltages, the crystals located on the edges of the cracks begin to disintegrate, and the resulting cracks deepen inward;
- Under the influence of periodic stresses, the crystals on the cracks rub against each other and that surface becomes smooth; As a result of the gradual growth of the cracks, the cross-sectional area decreases and, in connection with this, the value of the stress gradually increases, when the value of the stress reaches a dangerous level, the piezo element suddenly stops;
- The phenomenon of fatigue-induced degradation depends on the structure of molecules and crystals of the piezo element. Therefore, the assumption that the geometrical volume of the piezo element is completely filled (the assumption of the integrity of piezo elements) cannot be used in the interpretation of fatigue strength, etc.

The issue of calculating the fatigue degradation of piezoceramic piezo elements subjected to torsional deformation due to the effect of alternating stresses is considered to be one of the urgent issues in the design of piezoelectric motors. The development of modern technologies requires consideration of new factors (reasons) in these matters. One of the main factors here is the fatigue damage of piezo elements, that is, the formation and accumulation of defects of various types.

The gradual degradation process in piezo elements over time is associated with their long-term durability. Therefore, studying and researching the dissolution process is considered one of

the most urgent problems. The strength of piezo elements directly depends on the nature of the dissolution process occurring in the piezo elements of piezoelectric motors, making the study of the dissolution process a necessity.

The structure of the piezo element has a significant influence on the degradation process. For this reason, the degradation can be complex and unstable. Moreover, the dissolution process is strongly dependent on the influence of external factors. These can be the nature of loading, thermal regime, surface effects and other reasons. All these reasons affect the nature of the stress state of the piezo element. This, in turn, leads to disintegration. One type of breakdown is related to the arbitrary type of defects that originate and accumulate in the piezo elements, which is expressed by the term total damage. Such degradation is called scattered degradation. If the stress is homogenous (for example, in the tension of the rod), then the damage increases regularly with volume. If the stress field is heterogeneous, it is necessary to distinguish two stages for the analysis of the dissolution process: latent dissolution (incubation period) and apparent dissolution stages.

Microcracks and other defects are formed in the stage of latent degradation (in a certain time interval). At the moment of , local dispersion already occurs. Microcracks and other defects scattered around such local disintegration areas merge to form a macrocrack. For example, experiments conducted for the fatigue degradation of a piezo element indicate that in the initial stage of failure, damage accumulates continuously and the damage becomes a diffuse character. At the end of this stage, macrocracks are formed and they develop intensively in the next moments and the piezoelectric motor is damaged (Webber et al., 2017; Zhang & Gao, 2004; Koruza et al., 2018; Wei & Jing, 2017; Salazar et al., 2020).

Two types of approaches are used to investigate long-term dispersion problems. The first of these is the criterion approach. This type of approach is based on the creation of criteria that determine the long-term decay process of piezo elements. A measure known as “equivalent stress” is used to establish such criteria. An analytical review of studies using the criterion approach is given in (Akhmedov & Yusubova, 2022; Piriev, 2018). This approach is mostly used in problems of robustness investigation for time-independent stress tensor components.

3 A mathematical model of fatigue degradation of a cylindrical piezo element

As a result of numerous studies conducted on various piezo elements, L.M. Kachanov and Y.N.Rabotnov proposed a second approach, the “kinetic method”, for the study of long-term durability issues (Piriev, 2018). The basis of this approach is the inclusion of a function called the scalar “damage parameter”, which characterizes the state of the piezo element at an arbitrary value of the operating time t . The value of the included function corresponds to the initial state of the piezo element (before use), and the value corresponds to the state of complete disintegration of the piezo element (Piriev, 2023; Wang et al., 2016, 2018; Shibata et al., 2018; Webber et al., 2017; Zhang & Gao, 2004; Koruza et al., 2018; Wei & Jing, 2017; Salazar et al., 2020).

The description of a cylindrical piezo element made of a piezoceramic piezo element with outer and inner radius b , a , respectively, under the influence of a periodic normal force $F(t)$ and a torque $M(t)$ is as follows:

First of all, it is necessary to determine the damping coefficient corresponding to the forces acting on the piezo element:

The mass of the part with length dx of the piezo element with density ρ is:

$$dm = \rho A dx. \quad (1)$$

Here, A is the area of the ring formed in the cross section of the piezo element.

Denoting the displacement of the current section of the piezoelectric element along the axis by u , the following equation is obtained based on the equilibrium condition of the element dx :

$$\rho A \frac{\partial^2 u}{\partial t^2} = \frac{\partial N}{\partial x}.$$

From another side the element has an elongation as

$$\varepsilon = \frac{\partial u}{\partial x} = \frac{N}{EA}. \quad (2)$$

If $N = 0$ is subtracted from both obtained equations, then we obtain

$$\frac{\partial^2 u}{\partial x^2} = \frac{\rho}{E} \frac{\partial^2 u}{\partial t^2}, \quad (3)$$

where ρ is the density of the piezo element and E is the modulus of elasticity. In the obtained equation, the sought quantity u becomes a function depending on two free variables x and t .

Solution of the equation (3) is accepted as

$$u = X \sin(\omega_0 t), \quad (4)$$

where X is a function of only one free variable x and ω_0 is frequency of free oscillations. If considered (4) in equation (3) we have

$$\frac{d^2 X}{dx^2} + \frac{\rho \omega_0^2}{E} X = 0,$$

where

$$X = A \sin \sqrt{\frac{\rho \omega_0^2}{E}} x + B \cos \sqrt{\frac{\rho \omega_0^2}{E}} x. \quad (5)$$

The constants A and B are determined based on the boundary conditions. If it is assumed that the left end of the piezo element is fixed and the right end is free: $X = 0$, $x = 0$ and $\frac{dX}{dx} = 0$, $x = l$. Thus,

$$B = 0; \quad A \cos \sqrt{\frac{\rho \omega_0^2}{E}} l = 0.$$

The below formula

$$\omega_0 l \sqrt{\frac{\rho}{E}} = \frac{\pi}{2} (2n - 1)$$

is obtained from the last expression. Here, n is an arbitrary integer. This expression allows one to determine a series of successive values of the oscillation frequency specific to the length of the piezo element:

$$\omega_0 = \frac{\pi}{2l} (2n - 1) \sqrt{\frac{E}{\rho}}. \quad (6)$$

Thus, a piezoelectric element corresponding to the resonant state has an infinite number of oscillation frequencies.

In the elastic case, the law governing the period of change of tangent and normal stresses depending on time is as follows

$$\omega_0 = \frac{\pi}{2l} \sqrt{\frac{E}{\rho}}. \quad (7)$$

By substituting expression (6) into expression (5), it is possible to determine the form of oscillations corresponding to different values of n

$$X = A \sin \frac{(2n-1)\pi x}{2l}, \quad (8)$$

$$u = A \sin \frac{(2n-1)\pi x}{2l} \sin(\omega_0 t). \quad (9)$$

Depending on the values of n , different oscillation forms can be constructed using formulas (8) and (9). The emergence of different forms of oscillation is determined by the initial conditions of the excitation of a specific oscillation.

Similarly, using the equilibrium condition of moments of inertia and internal forces during the torsion of the piezo element: the differential equation of torsional oscillations is written as follows

$$\frac{\partial^2 \varphi}{\partial t^2} = \frac{GJ_0}{I_0} \frac{\partial^2 \varphi}{\partial x^2}, \quad (10)$$

where I_0 is the mass moment of inertia per unit length, J_0 is the polar moment of inertia of the cross section, G is the modulus of elasticity in sliding, and ϕ is the angle of rotation formed during the torsion of the cylindrical piezo electric element.

Since the height deformation in the piezo element driving the piezoelectric motors is much smaller than the torsional deformation, it will be assumed here that the collapse occurs due to the torsional stress. For this purpose, using the dynamic coefficient of the system, the stress in the cross-section of the piezo element can be written as follows

$$\tau_d = \beta \tau_s, \quad (11)$$

where τ_d is the tangential stress caused by the excitation force in the cross section of the piezo-electric element, τ_s is the stress caused by the static effect of the maximum value of the excitation force, and β is the dynamic coefficient of the system and is shown in (Figure 1).

$$\beta = \frac{1}{1 - \left(\frac{\omega}{\omega_0}\right)^2}, \quad (12)$$

where ω is the frequency of the exciting oscillation. If the comparison of frequencies ω and ω_0 shows that there is a danger of resonance, depending on the conditions, one of the frequencies can be changed by making a simple design change.

The amplitude value of the exciting stress during torsion is given as:

$$\tau_s = \frac{M}{J_r} r \quad (13)$$

where r is the current radius. Substituting (13) into (11) yields the dynamic stress

$$\tau_d = \beta \cdot \frac{M}{J_r} r. \quad (14)$$

Here, r represents the current radius, and J_r denotes the moment of inertia at the cross-section

$$J_r = \frac{\pi}{2}(b^4 - a^4). \quad (15)$$

As seen from equation (13), the maximum induced stress on the outer surface ($r=b$) of the piezo element is given by the formula

$$\tau_{s,\max} = \frac{M}{W_k}; W_k = \frac{\pi a^4}{2b} \left(\left(\frac{b}{a}\right)^4 - 1 \right), \quad (16)$$

where W_k represents the torsional resistance moment.

Considering the degradation criterion as follows

$$\tau_s + K^* \tau_s = \frac{\tau_0}{\beta}, \quad (17)$$

where τ_0 represents the sudden strength limit, K^* is the damage operator, and in the case of monotonous increase in loading process, the self-elasticity takes the form of an integral operator (Akhmedov & Yusubova, 2022; Piriev, 2018, 2023; Wang et al., 2016)

$$K^* \tau_s = \int_0^t K(t - \xi) \tau_s(\xi) d\xi. \quad (18)$$

Here, $K(t - \xi)$ is called the damage kernel.

The initial degradation time and the equation for the degradation front will be derived from degradation criterion (17). For this purpose, if (18) is expressed in the strength criterion (17), the following integral equation is obtained

$$\tau_s(t, t) + \int_0^t K(t - \xi) \tau_s(\xi) d\xi = \frac{\tau_0}{\beta}. \quad (19)$$

The initial degradation will occur on the outer surface ($r = b$) of the piezo element, where the maximum tensile stress is present. The initial degradation time t_1 is referred to as the hidden degradation time of the piezo element, and to find this time, equation (16) is considered in (17)

$$\frac{M}{W_k} (1 + K^* \cdot 1) = \frac{\tau_0}{\beta}. \quad (20)$$

From equations (18) and (20), the following equality is obtained

$$\int_0^{t_1} K(\xi) d\xi = \frac{\tau_0 W_k}{\beta M} - 1. \quad (21)$$

Since the hidden degradation time is positive, the right side of equation (21) must also be positive. Using this condition, the restriction for the intensity of the moment M is determined as follows

$$M < \frac{\tau_0 W_k}{\beta M}. \quad (22)$$

In cases, where the value of the torsional moment is greater than $\frac{\tau_0 W_k}{\beta M}$, the degradation will occur suddenly. Therefore, it is assumed that condition (22) is satisfied in subsequent stages of solving the problem.

To derive an explicit formula for the incubation period depending on the type of damage kernel, the latent degradation times for the three damage kernel cases (constant, exponential, and singular) are determined using (21)

$$\begin{cases} K(t - \xi) = K_0 = \text{const} & t_1 = \frac{1}{K_0} \left(\frac{\tau_0 W_k}{\beta M} - 1 \right) \\ K(t - \xi) = K_0 e^{-m(t-\xi)} & t_1 = \frac{1}{m} \left[1 - \frac{K_0}{m} \left(\frac{\tau_0 W_k}{\beta M} - 1 \right) \right]^{-1} \\ K(t - \xi) = K_0 (t - \xi)^{-\alpha}, \quad 0 < \alpha < 1 & t_1 = \left[\frac{1 - \alpha}{K_0} \left(\frac{\tau_0 W_k}{\beta M} - 1 \right) \right]^{\frac{1}{1-\alpha}} \end{cases}. \quad (23)$$

After the initial fracture, a crack zone forms on the outer surface of the piezo element (Figure 1).

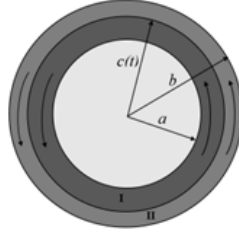


Figure 1: Diagram of the cross-section of the piezo element.

The boundary between the distribution area and the undistributed area is called the distribution front (Wang et al., 2018). The character of the movement of the distribution front determines the intensity of the evolving dispersed distribution process. It is assumed that the work capacity of the piezo element in front of the distribution front is completely lost. After the distribution front is formed, the section of the piezo element consists of two regions. The first is the region in the form of a ring with an internal radius a and an external radius $c(t)$ (undistributed part), and the external region, called the distribution area, has an internal radius $c(t)$ and an external radius b . For both regions, the moment of inertia is determined as

$$J_1 = \frac{\pi}{2} (c^4(\xi) - a^4), \quad (24)$$

$$J_2 = \frac{\pi}{2} (b^4 - c^4(\xi)). \quad (25)$$

Using these formulas and (13), the following equations for the tensile stresses in both regions are obtained

$$\tau_{st}^{(1)} = \frac{2M_1(\xi)}{\pi b^3 (f^4(\xi) - f_0^4)} f(t), \quad (26)$$

$$\tau_{st}^{(2)} = \frac{2M_2(\xi)}{\pi b^3 (1 - f^4(\xi))} f(t). \quad (26)$$

Here, the dimensionless quantities are defined as follows

$$f(\xi) = \frac{c(\xi)}{b} \quad ; \quad f(t) = \frac{r(t)}{b} \quad ; \quad f_0 = \frac{a}{b}.$$

The stiffness of the piezo element is characterized by the relative torsion angle θ . The torsion angle per unit length is called the relative torsion angle and is expressed as

$$\theta = \frac{M}{GJ_r}. \quad (27)$$

It is assumed that the elastic modulus of the internally twisted region is G_1 , and the externally distributed region is G_2 . When the piezo element is subjected to the torsion moment $M(t)$, the torsion moments carried by the internal and external regions are denoted as $M_1(t)$ and $M_2(t)$ respectively, so that

$$M(t) = M_1(t) + M_2(t). \quad (28)$$

Since both regions work equally, the relative torsion angles must be equal, i.e.

$$\theta_1 = \theta_2. \quad (29)$$

From equations (27) and (29), and considering that the internal region is subjected to inheritance type damage, we obtain

$$\frac{1}{G_1^*} \cdot \frac{M_1(\xi)}{J_1(\xi)} = \frac{M_2(t)}{G_2 J_2(t)}. \quad (30)$$

Here,

$$\frac{1}{G_1^*} = \frac{1}{G_1}(1 + K^*). \tag{31}$$

Substituting (31) into (30), the following equality is obtained (Piriev, 2018)

$$\frac{1}{G_1}(1 + K^*) \cdot \frac{M_1(\xi)}{f^4(\xi) - f_0^4} = \frac{M_2(t)}{G_2(1 - f^4(t))}, \tag{32}$$

where

$$K^* \cdot \frac{M_1(\xi)}{f^4(\xi) - f_0^4} = \int_0^t K(t - \xi) \cdot \frac{M_1(\xi)}{f^4(\xi) - f_0^4} d\xi. \tag{33}$$

From equations (32) and (33), the following integral equation is obtained

$$g \left(\frac{M_1(\xi)}{f^4(t) - f_0^4} + \int_0^t K(t - \xi) \cdot \frac{M_1(\xi)}{f^4(\xi) - f_0^4} d\xi \right) = \frac{M_2(t)}{1 - f^4(t)}, \tag{34}$$

where $g = \frac{G_2}{G_1}$.

After determining $M_2(t) = M(t) - M_1(t)$ from (28), substituting the obtained expression into (34), (26), and (19), the following system of integral equations is obtained

$$\begin{cases} \frac{\tilde{M}(t)}{f^4(t) - f_0^4} + \int_0^t K(t - \xi) \frac{\tilde{M}(t)}{f^4(\xi) - f_0^4} d\xi = \frac{1 - \tilde{M}(t)}{g(1 - f^4(t))}, \\ \frac{\tilde{M}(t)}{f^4(t) - f_0^4} + \int_0^t K(t - \xi) \frac{\tilde{M}(t)}{f^4(\xi) - f_0^4} d\xi = \frac{\gamma}{f(t)}, \end{cases} \tag{35}$$

where

$$\tilde{M}(t) = \frac{M_1(t)}{M(t)}; \quad \gamma = \frac{\pi b^3 \tau_0}{2\beta M}$$

are the introduced dimensionless quantities. By subtracting the equations in system (35) side by side, the dimensionless torsional moment $\tilde{M}(t)$ is found as:

$$\tilde{M}(t) = \frac{f(t) - \gamma g(1 - f^4(t))}{f(t)}. \tag{36}$$

Considering (36) in the second equation of (35), the following integral equation is obtained

$$\frac{f(t) - \gamma g(1 - f^4(t))}{f(t)(f^4(t) - f_0^4)} + \int_0^t K(t - \xi) \frac{f(\xi) - \gamma g(1 - f^4(\xi))}{f(\xi)(f^4(\xi) - f_0^4)} d\xi = \frac{\gamma}{f(t)}. \tag{37}$$

It is clear that the maximum value of the function $f(t)$ is unity. However, for some interval values of $f(t)$, at a given moment in time, the velocity of motion of the dispersion front determined by its derivative may be zero. This moment is precisely considered as the final or complete dispersion time.

Equation (37) expressing the motion of the dispersion front is called the second type Volterra non-linear integral equation. Solving this equation for the general form of the kernel of the integral presents a complex mathematical problem. However, obtaining the solution of the integral equation in an explicit analytic form is possible for relatively simple special cases of kernels. Such an approach allows analyzing the quality of the studied dispersed dispersion process and determining its characteristic properties. Therefore, initially assuming the kernel as $K(t - \xi) = 1$, the equation is differentiated with respect to t on both sides, yielding:

$$\frac{df}{dt} = - \frac{f(f^4 - f_0^4)(f - \gamma g(1 - f^4))}{f(1 + 4\gamma g f^3)(f^4 - f_0^4) - (5f^4 - f_0^4)(f - \gamma g(1 - f^4)) + \gamma(f^4 - f_0^4)^2}. \tag{38}$$

Similarly, for the exponential kernel $K(t - \xi) = e^{-m(t-\xi)}$, the differential equation is obtained by differentiating with respect to t :

$$\frac{df}{dt} = -\frac{mf(f^4 - f_0^4) [\gamma(f^4 - f_0^4) - (f - \gamma g(1 - f^4))]}{f(1 + 4\gamma g f^3)(f^4 - f_0^4) - (5f^4 - f_0^4)(f - \gamma g(1 - f^4)) + \gamma(f^4 - f_0^4)^2} \quad (39)$$

For differential equations (38) and (39), the dimensionless initial condition is given by

$$f(t = t_1) = 1. \quad (40)$$

Since equations (38) and (39) are ordinary differential equations, numerical methods are used for their solution. One such method is the Runge-Kutta method. In MATLAB, there are two built-in functions for solving differential equations using the Runge-Kutta method: "ode23" and "ode45". The "ode23" function represents second and third order Runge-Kutta integration, while the "ode45" function utilizes fourth and fifth order Runge-Kutta integration.

To analyze the development of the fracture surface, $\beta = 5.26$ is taken for the dynamic factor in equation (23) and $t_1 = 3$ is chosen. Equation (38) is then solved with the initial condition $f(t_1) = 1$, considering the thickness of the piezoelectric element wall, using the MATLAB "ode45" function. This provides deviations characterizing the expansion of the fracture surface, which are depicted in Figure 2.

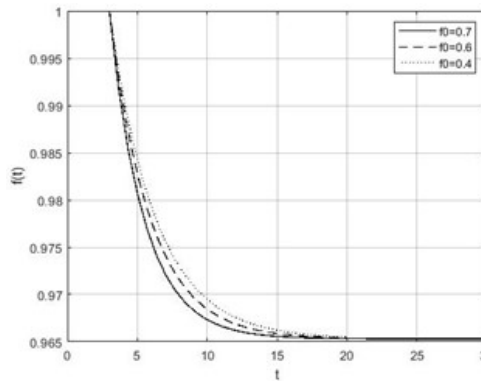


Figure 2: Deviation of the fracture surface

The analysis of Figure 2 shows that as the thickness of the piezoelectric element wall increases, the speed of the fracture surface decreases. This is consistent with the fact that when the thickness of the wall is large, its resistance to external forces increases, thus prolonging the fracture process.

The influence of the thickness of the piezoelectric element wall with $f_0 = 0.7$ on the dynamic factor's effect on the fracture speed is depicted in Figure 3. As seen from Figure 3, an increase in the dynamic factor leads to a sharp increase in the fracture speed.

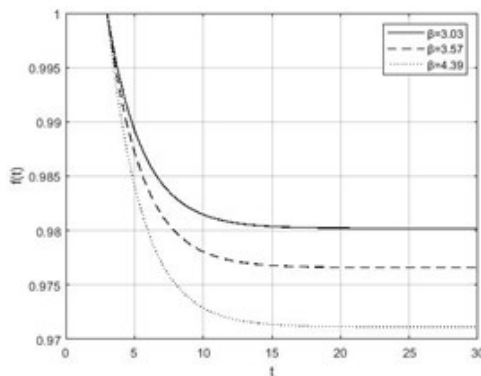


Figure 3: Deviations in the movement of the fracture surface

For the values $f_0 = 0.7$ and $\beta = 3.03$ of the piezoelectric element wall thickness, the effect of the parameter m on the fracture process is given in Figure 4.

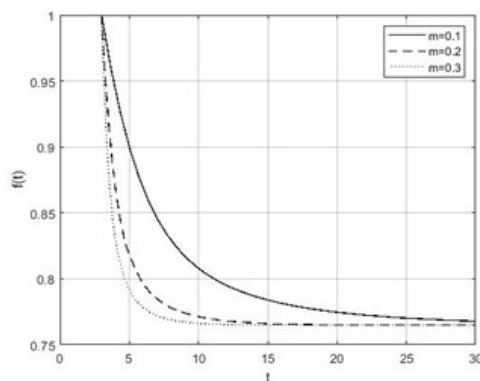


Figure 4: Fracture surface deviations

As seen from Figure 4, in the case of an exponential kernels, the parameter m has a certain influence on the fracture of the piezoelectric element. Specifically, an increase in the value of this parameter accelerates the expansion of the fracture surface at certain intervals of time.

4 Conclusion

The mathematical model is developed and solved for the formation and development of the fracture zone during the torsion of cylindrical piezo elements, which are one of the main elements of micro piezo motors. The problem was examined under the assumption of constant elasticity modulus. Additionally, formulas for the incubation period and integral equations for the motion of the fracture surface are derived. Specific cases are analyzed for their qualitative characteristics. In general, deviations representing the movement of the fracture surface are formulated using numerical calculation methods.

References

- Akhmedov, N.K., Yusubova, S.M. (2022). Investigation of elasticity problem for the radially inhomogeneous transversely isotropic sphere. *Mathematical Methods in the Applied Sciences*. doi: <https://doi.org/10.1002/mma.8360>
- Gayvorovskaya, G.S., Rybalov, B.A. (2015). Features of optical signal switching when using different modes of information transmission. *Holodilna Tekhnika ta Tekhnolohiia*, 51(6), 100-106. Odessa. Retrieved from http://nbuv.gov.ua/UJRN/htit_2015_51_6_18
- Hasanov, M.H., Gardashov, S.G. (2017). Frequency matching of dimensions of piezoelectric motor elements for optical switches. *Reliability and Quality of Complex Systems*, 4, 49-55.
- Hasanov, M.H. (2018). Piezoelectric Optical Deflector With Adaptive Mirror. *T-Comm*, 6, 56-60.
- Hasanov, M.H. (2019). Photon switch of full optical networks. *T-Comm*, 13(8), 47-51.
- Hasanov, M.H., Agayev, N.B., Atayev, N.A., & Fataliyev, V.M. (2021). A new generation of controlled optic switch. *T-Comm*, 15(3), 63-68.
- Hasanov, M.H., Akhmedov, N.K., Bashirov, R.J., Piriev, S.A., Boiprav, O., & Ismailov, N.E. (2024). The development of a piezoelectric defect detection device through mathematical modeling applied to polymer composite materials. *New Materials, Compounds and Applications*, 8(1), 62-74.

- Hasanov, M.H., Hacıyeva, K.R., & Qodjaeva, S.F. (2022). Multifunctional adaptive piezoelectric switch of optical channels. *T-Comm. Telecommunications and Transport*, 13(29), 64-69.
- Koruza, J., Bell, A.J., Frömling, T., Webber, K.G., Wang, K., & Rödel, J. (2018). Requirements for the transfer of lead-free piezoceramics into application. *J. Materiomics*, 4, 13–26. doi: 10.1016/j.jmat.2018.02.001.
- Lokoshchenko, A.M. (2016). *Creep and Creep Rupture of Metals*. 1st ed. Moscow, Russia: Fizmatlit.
- Piriev, S.A. (2018). Long-term strength of a thick-walled pipe filled with an aggressive medium, with account for damageability of the pipe piezo element and residual strength. *Journal of Applied Mechanics and Technical Physics*, 59(1), 163–167.
- Piriev, S.A. (2023). Scattered Destruction of a Cylindrical Isotropic Thick Pipe in an Aggressive Medium with a Complex Stress State. *Engineering Cyber-Physical Systems and Critical Infrastructures*, 7, 383-395.
- Ryabtsov, A.V. (2013). Piezooptical scanning switches. *Information Theories and Applications*, 20(3), 295-299.
- Salazar, R., Serrano, M., & Abdelkefi, A. (2020). Fatigue in piezoelectric ceramic vibrational energy harvesting: A review. *Applied Energy*, 270, 115-161. doi: 10.1016/j.apenergy.2020.115161.
- Samarin, A. (2006). Miniature linear piezoelectric motors. *Components and Technologies*, 10, 6. Retrieved from https://kit-e.ru/wp-content/uploads/2006_10_36.pdf
- Shibata, K., Wang, R., Tou, T., & Koruza, J. (2018). Applications of lead-free piezoelectric materials. *MRS Bull.*, 43, 612–616. doi: 10.1557/mrs.2018.180.
- Vishnevsky, V.S. (1993). Piezoelectric reversible drive. Patent No. 1827708. Russian Federation. Inventors: Kurilko, A.A., Matviychuk, D.A., Vishnevsky, D.V., Gasanov, M.G.
- Wang, C., Zhu, Y., Li, X., & Gao, R. (2016). Low Cycle Fatigue Behavior of SnAgCu Solder Joints. *Rare Metal Materials and Engineering*, 45(4), 829–835.
- Wang, H., Jasim, A., & Chen, X. (2018). Energy harvesting technologies in roadway and bridge for different applications - A comprehensive review. *Applied Energy*, 212, 1083-1084.
- Webber, K.G., Vögler, M., Khansur, N.H., Kaeswurm, B., Daniels, J.E., & Schader, F.H. (2017). Review of the mechanical and fracture behavior of perovskite lead-free ferroelectrics for actuator applications. *Smart Mater Struct.*, 26, 063001. doi: 10.1088/1361-665X/aa590c.
- Wei, C., Jing, X. (2017). A comprehensive review on vibration energy harvesting: Modelling and realization. *Renewable and Sustainable Energy Reviews*, 74, 1-18.
- Zhang, T.Y., Gao, C.F. (2004). Fracture behaviors of piezoelectric materials. *Theor. Appl. Frac. Mech.*, 41, 339–379. doi: 10.1016/j.tafmec.2003.11.019.